ChemPubSoc Europe

DOI: 10.1002/celc.201801146

CHEMELECTROCHEM Articles

Towards more Durable Electrochemical Capacitors by Elucidating the Ageing Mechanisms under Different Testing Procedures

Minglong He,[a] Krzysztof Fic,*[b] Elżbieta Frąckowiak,[b] Petr Novák,[a] and Erik J. Berg*[a, c]

Electrical double-layer capacitors (EDLCs) commonly denoted supercapacitors are rechargeable energy storage devices with excellent power and energy delivery metrics intermediate to conventional capacitors and batteries. High-voltage aqueous electrolyte based EDLCs are particularly attractive due to their high-power capability, facile production, and environmental advantages. EDLCs should last for thousands of cycles and evaluation of future cell chemistries require long-term and costly galvanostatic cycling. Voltage holding tests have been proposed to shorten evaluation time by accelerating cell degradation processes. Whether voltage holding can replace cycling completely remains undemonstrated. In this work, a systematic investigation of the influence of testing procedure on cell performance is presented. The state-of-the-art *post-mortem* and *operando* experimental techniques are implemented to elucidate ageing mechanisms and kinetics inside EDLC cells under different testing procedures. Carbon corrosion occurring on the positively polarized electrode leads to the lower active surface area and higher oxygen content. On the contrary, an increase of surface area and micropore volume are observed on the negatively polarized electrode. Repeated galvanostatic cycles at $U < 1.6$ V appears to facilitate the depletion of oxygen species on the positively polarized electrode in comparison with voltage holding, which indicates a more complex degradation mechanism during cycling. Caution is advised when comparing results from different test procedures.

1. Introduction

Electrical double-layer capacitors (EDLCs), also often called electrochemical capacitors or supercapacitors (in fact – the latter is not recommended), demonstrate a high specific power (in W/kg), but moderate specific energy (in Wh/kg) in comparison with Li-ion batteries and other redox-based technologies.[1–2] Electrostatic type of energy storage and lack of the structural changes in the electrode material ensures excellent cycle life of $>100\,000$ cycles, which is much higher than for Li-ion batteries ($<5\,000$ cycles).[3–9] The further development of EDLCs is today oriented towards enhancement of gravimetric/volumetric energy[10–13] while retaining their high cyclability. Among the various approaches proposed to date,[6,14–18] hybrid concepts such as merging advantages of Li-ion and capacitive technologies appear suitable for applications requiring energy storage, but with strict space/mass limitations.[19–24] Although the specific and volumetric energy density can be remarkably improved,[25] their cyclability and impact on the environment is still unsatisfactory. For that reason, carbon-based capacitors with aqueous electrolytes characterized by moderate specific energy, but long cycle life, are recognized as interesting systems.[26–28] By definition, electrostatic attraction of ions at the electrode/electrolyte interface should not affect the electrode properties and the performance fade over cycling should be negligible. In the real systems, however, electrode damage, loss of electric contact between active material and current collector, electrolyte decomposition, parasitic reactions and many other factors contribute to the gradual capacitor failure.[29] As the limits of purely capacitive energy storage seem to be reached,[6,9–10,30–34] identifying and understanding the reasons of performance fade is one of the most critical issues in further development of capacitor technology.[35–39] Nonetheless, ageing investigations are time-consuming and usually hamper the development EDLCs and require a testing time for several thousands of cycles to determine the lifetime.[35] Cell lifetime is generally accepted to end when either 20% of capacitance loss or initial resistance increase by 100% has occurred.[40]

Several procedures have been proposed in order to increase the time efficiency and accelerate the ageing of EDLCs for cycle-life evaluations.[35,41–42] Floating tests[43] have among the various approaches been widely employed to study EDLC

[a] Dr. M. He, Prof. P. Novák, Dr. E. J. Berg
Electrochemistry Laboratory
Paul Scherrer Institut
5232 Villigen, Switzerland
[b] Dr. K. Fic, Prof. E. Frąckowiak
Institute of Chemistry and Technical Electrochemistry, Poznan University of Technology, 60-695 Poznan, Poland
E-mail: krzysztof.fic@put.poznan.pl
[c] Dr. E. J. Berg
Department of Chemistry
Uppsala University
751 21 Uppsala, Sweden
E-mail: erik.berg@kemi.uu.se

Supporting information for this article is available on the WWW under https://doi.org/10.1002/celc.201801146

ageing, either by simply holding a constant maximum voltage U_{max} or by mixing voltage holding and galvanostatic cycling.[29,35,42,44–46] For instance, Weingarth et al. compared the ageing efficiency of voltage holding test and respective galvanostatic cycling test on EDLCs with an ionic liquid electrolyte [EMIM][BF_4].[40] They demonstrated that EDLCs could maintain the capacitance over 12000 cycles between 0–3.75 V, while the capacitance fading is clearly observed after the voltage holding process at $U = 3.75$ V for 300 hours. On the contrary, results of Avasarala et al. and our previous study suggested that repeated cycling seems to be more harmful to the electrode integrity compared to the floating test.[47–48] The formation and removal rates of oxygen-containing surface species appeared to be higher during cycling compared to floating tests and were current-dependent, e.g., the degradation was pronounced under constant current conditions.

Whether floating test and cycling test lead to the same ageing processes is hitherto unknown and intensively debated. Definitely, both techniques provoke the performance fade, but different phenomena contributing to the final system failure might be stimulated and the conclusions are not comparable. The most insightful approach would require the application of both techniques but considering the time-consuming character of these investigations a selection between the two is usually necessary. On the one hand, electrochemical capacitors are supposed to operate over thousands of cycles; hence, typical cycling procedures appear to be the most appropriate. On the other hand, their high-power performance is demonstrated at high voltages, which could be exploited in practical systems, thus closer mimicking the floating test operation conditions. The time at high voltage during cycling is certainly shorter than for the floating and a fully reversed polarization during discharge might restore the system and prolong the cycle life. The nature, rate, onset potential, and extent of various degradation mechanisms involving both the electrode and the electrolyte under both cycling and floating need to be further investigated. Although the failure modes of non-aqueous EDLCs have been already well addressed in the literature,[29,36,44,49] there is a general lack of understanding the ageing phenomena of aqueous electrolyte based EDLCs.

The aim of present work is to elucidate ageing processes and evaluate the long-term stability of aqueous EDLCs under galvanostatic cycling and floating test procedures by employing state-of-the-art *post-mortem* and *operando* experimental techniques. In our study, we have reported for the first time the differences in the internal pressure variation (*operando*), dependently on the procedure applied. Furthermore, we have examined the electrode textural properties after various ageing procedures. It is demonstrated that modifications of one technique (like current load) might provoke different ageing mechanisms.

Experimental

Materials and Cell Assembly

Carbon electrodes were prepared from the activated carbon fabric (ACC 507-20, Kynol, Germany) with diameters of 14 mm ($m = 18 \pm 0.3$ mg) for *operando* pressure cell analysis and 18 mm ($m = 30 \pm 0.3$ mg) for Online Electrochemical Mass Spectrometry (OEMS) cell analysis, respectively. The employed electrolyte was 1 mol/L Li_2SO_4, which was prepared by dissolving analytical quality Li_2SO_4 salt (> 99.99%, Sigma-Aldrich, Switzerland) in distilled water. The cells were assembled in a symmetric configuration containing two identical activated carbon electrodes, a layer of glass fiber separator (Whatman GF/C), and a fixed amount of 1 mol/L Li_2SO_4 electrolyte (0.2 mL for pressure analysis cell and 0.25 mL for the OEMS cell).

The Cycling and Voltage Holding Test Procedure

Cycling and voltage holding protocols were pursued with a precision computer controlled potentiostat/galvanostat (CCCC hardware, Astrol Electronic, Switzerland). The galvanostatic cycling tests at either 0.2A/g or 0.5 A/g were performed in a cell voltage window of 0–1.6, 0–1.8, and 0–2.0 V. The voltage holding tests were applied with a cut-off voltage at 1.6, 1.8, and 2.0 V. In addition, accelerated ageing protocol combining the galvanostatic cycling (0.2 A/g) with voltage holding process (cut-off at 1.6, 1.8, and 2.0 V) was applied in order to simulate the practical ageing process.[42] Please note, the employed carbon electrode material and the short-term electrochemical response of symmetric EDLCs based on the same lithium-sulfate aqueous electrolyte were already well characterized by us[47, 50-51] and others.[42, 46]

It should be pointed out that in the test performed in the study, the final state of health of the capacitor was different, since we decided to perform all the testing procedures with no limit for end-of-life criteria. Such approach allowed us to eliminate the influence of the experiment time (to be further compared between the techniques and the cut-off voltages). Furthermore, it allowed for elucidation of the dynamics of the performance fade after reaching the standard end-of-life criteria.

Post-Mortem Electrode Analysis

In order to perform the *post-mortem* electrode analysis, symmetric EDLC cells were disassembled in ambient environment after either cycling or floating test. Carbon electrodes were taken out from the cell and then washed with distilled water to remove the residual electrolyte. Afterwards, washed carbon electrodes were dried at 120 °C under vacuum for 12 hours before the electrode characterization.

The characterization methods of carbon electrodes have been presented in our previous studies.[47,50–51] In brief, nitrogen adsorption isotherms of activated carbon electrodes were measured by ASAP 2020 analyzer (Micromeritics, USA) at 77K. Specific surface areas of carbon were estimated by applying Brunauer-Emmett-Teller (BET) models. Pore size distribution and pore volumes were computed with non-local density functional theory (2D NL DFT) method.[52–53] Temperature-programmed desorption (TPD) method was employed to characterize surface functionalities of activated carbon after cell ageing.[46–47] Elemental analysis (VarioMicroCube, Elementar, Germany) indicated the carbon and oxygen content in pristine and *post-mortem* electrodes.

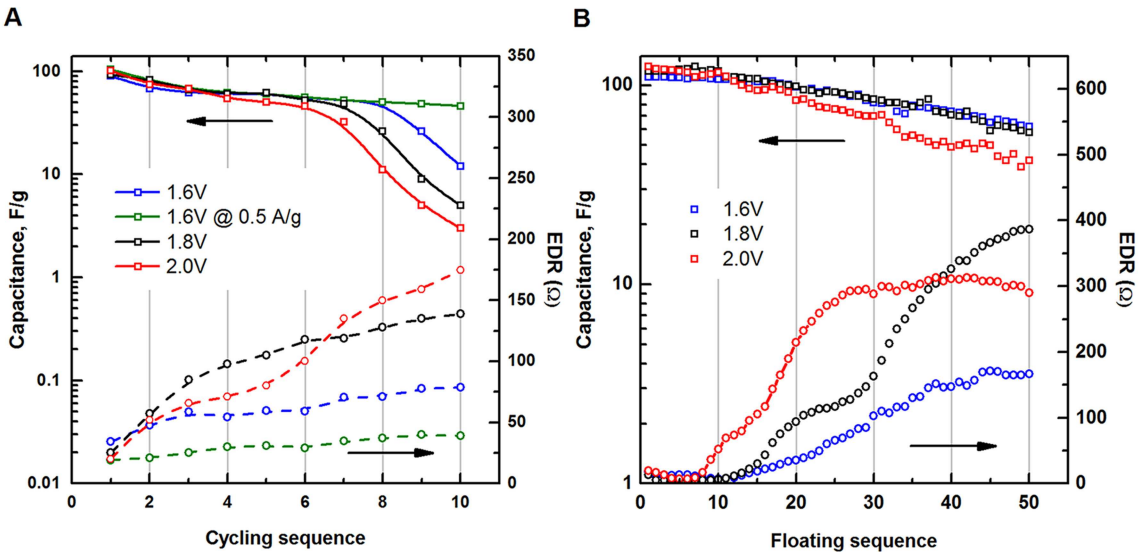

Figure 1. Capacitance and EDR evolution profiles for EDLCs aged under (A) cycling at 0.2 A/g and (B) voltage holding conditions at cut-off voltages U_{max} of 1.6 (blue hollow square and circle), 1.8 (black hollow square and circle), and 2.0 V (red hollow square and circle), respectively. Capacitance and EDR evolution profiles of EDLCs cycling at 0.5 A/g are also included (green hollow square and circle). 1 cycling sequence = 1000 charge/discharge cycles and 1 floating sequence = 2 hours voltage holding at U_{max}.

Operando gas Analysis

The components and working principles of the *operando* gas analysis techniques have been introduced elsewhere.[47,51,54–55] Briefly, an *operando* pressure analysis cell has two major components, i.e., an electrochemical cell and a pressure transducer. The electrochemical cell is a coin type cell in which the internal cell pressure is continuously measured by a pressure sensor. OEMS set-up is based on an electrochemical cell (also noted as OEMS cell) and a mass spectrometer (MS). Unlike the pressure analysis cell, OEMS cell has an open cell configuration, allowing Ar gas flows through the cell and carries the electrochemically evolved gas species to the MS. For all *operando* gas analysis, 3 hours of equilibrium time was fixed and set before electrochemical cycling in order to obtain a stable background.

2. Results and Discussion

Long-term cell performance evaluations were pursued in order to investigate the behaviour of EDLCs subjected to accelerated ageing test protocols, such as electrochemical galvanostatic cycling or floating conditions.

The development of capacitance and equivalent distribution resistance (EDR) were monitored during either 10 cycling sequences (Figure 1A, 1 sequence = 1000 charge/discharge cycles) or 50 floating sequences (Figure 1B, 1 sequence = 2 hours voltage holding at U_{max}). Under the electrochemical cycling conditions (0.2 A/g), the initial specific capacitance of 106 F/g is reduced by 20% after the second sequence (ca. 450 h) and an accelerated capacitance fading occurs after 4 sequences. The fading rate depends as expected on the applied cut-off voltage U_{max}: the higher the U_{max}, the stronger the driving force for detrimental electrochemical side-reactions (as further investigated below) and the shorter the EDLC cycle lifetime. The capacitance retention could be markedly improved - while maintaining the same U_{max} – simply by increasing the applied charge/discharge current (0.5 A/g, Figure 1A), thus reducing the time during which the EDLC is exposed to high cell polarizations. Although a high current load might provoke electrode damage caused by temperature increase, binder decomposition, etc., several side reactions of faradaic origin may be suppressed by their insufficient kinetics. The capacitance loss could largely be related to increase in cell impedance as both the EDR and equivalent series resistance (ESR) profiles (Figure S1A,B in supplementary information) were observed to correlate with the cell capacitance. One should however note that the initial capacitance fade is noticeably slower while a well-pronounced ESR increase is observed. Possibly a structural change of the electrode occurs initially involving electrode potential equilibration and hydrogen electrosorption, which will be discussed further below.

Under the electrochemical floating conditions, the initial specific capacitance of 106 F/g is reduced by 20% already after 60 hours (as compared to ca. 450 hours during cycling conditions). Generally, it has already been concluded in previous studies that holding the voltage at high cell polarizations for extended periods of time clearly deteriorates the cell performance more time-dependent compared to normal cycling in the same voltage window.[42,46]

It might be concluded that the capacitance drop does not follow the changes of the EDR straightforwardly, hence, the reason of the performance fade must be different. For instance, the capacitance decay for all cut-off voltages is similar for initial sequences of cycling and floating, however, the evolution of EDR is dramatically different. Interestingly, the performance for the cut-off voltage of 1.6 V reached by 0.2 and 0.5 Ag^{-1} reflects different profile for EDR development. It clearly indicates that

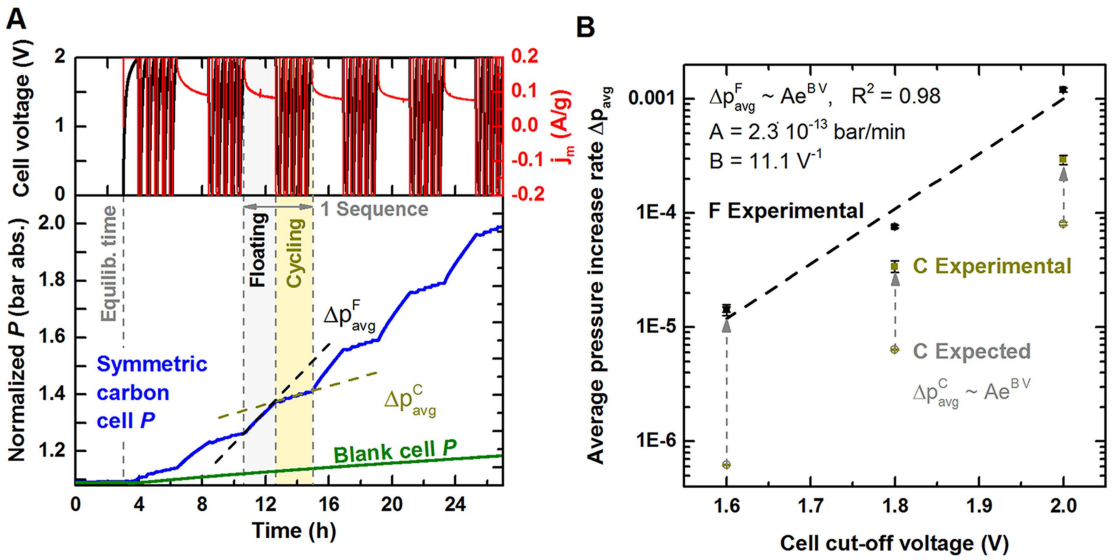

Figure 2. (A) Cell voltage (black solid lines), specific current (red solid lines), internal pressure (blue solid lines) profiles during accelerated ageing process proceeded with 5 galvanostatic cycles (0.2 A/g) and a floating voltage of 2.0 V at room temperature. Besides, the internal pressure profile of the EDLC cell without activated carbon electrode (Blank cell, green solid line) is included. (B) Correlation between the average pressure increase rate ΔP_{avg} and the cell cut-off voltage.

higher current load is less harmful for the capacitor performance because of the higher ohmic drop during polarization change. This tendency has been preserved till the end of the cycling sequence. This furthermore suggests that the capacitor state of health is different at the end of the sequence. This observation must be followed by the post-mortem analysis of the electrodes in order to evaluate the loss of the specific surface area and oxygen content, assumed to differ significantly.

As expected, the most dramatic capacitance decay has been observed for the capacitor cut-off voltage of 2.0 V (after 6th cycling sequence). The capacitance loss was accompanied by the remarkable increase of the EDR, most likely caused by the internal pressure increase. Similar tendency was observed for the floating test – the EDR started to increase after 10th voltage hold sequence.

Similarly to the conclusions above, the higher the holding voltage, the stronger the driving force for electrochemically initiated side-reactions and the more rapid the capacity fade. However, when comparing the evolution of the capacitance and impedance of the cells, several important differences are observed. First, capacity loss and impedance increase initiate immediately upon cycling (Figure 1A), while the cell performance during floating remains virtually constant during the first ~10 floating sequences.

Secondly, both the capacitance loss and cell impedance display a monotonic increase during cycling whereas the impedance appears to level off during floating in spite of a continuous capacity fade. In conclusion, several adverse side-reactions are at play during high cell polarizations, which are most likely different in both nature and extent during the electrochemical cycling and floating conditions. In order to investigate these ageing processes further, we investigated the gas evolution inside the cell by *operando* pressure measurements.

Figure 2A presents the voltage and current profiles along with the internal pressure development of the EDLC subjected to a mixed accelerated ageing test. Each sequence is based on five galvanostatic cycles (0.2 A/g, $0 < U < 2.0$ V) combined with a potentiostatic step at 2.0 V for 2 hours, during which the leakage current is recorded. The corresponding 1.6 V and 1.8 V cut-off voltage experiments are shown in Figure S2. Cell pressure increases immediately after the equilibration time as a result of electrochemically initiated gas evolution. The evolving gases were previously mainly observed to be H_2, CO_2 and CO and predominantly originate from carbon corrosion and electrolyte degradation reactions as described elsewhere.[47] There is a qualitative difference in the gassing behaviour during the cycling and floating steps. For instance, rapid pressure fluctuations are observed due to gas evolution/consumption reactions during charge/discharge cycling (Figure 2A, and in *dP/dt* in Figure S2 in supplementary information), whereas a single gas evolution reaction appears to prevail during floating.[47] The OEMS measurement merely confirms this and previous data (Figure S3A,B); regardless of the cut-off voltage, gas evolving signals of CO and CO_2 are detected in a fluctuation pattern during cycling. An exponential decay of gas evolution rate occurring under the voltage holding is in a line with the leakage current profile. In order to quantitatively evaluate the impact of either floating or cycling on the pressure increase rate we extracted the average irreversible pressure increase rate Δp^F and Δp^C during several floating and cycling steps (Figure 2A), respectively, and plotted the results *vs.* cell cut-off voltage (Figure 2B). The average pressure increase rate Δp_{avg} (in bar/min) is expected to be proportional to the average gas generation rate Δn (in mol/min) via the ideal gas law (*Vol*, *R*, *T*

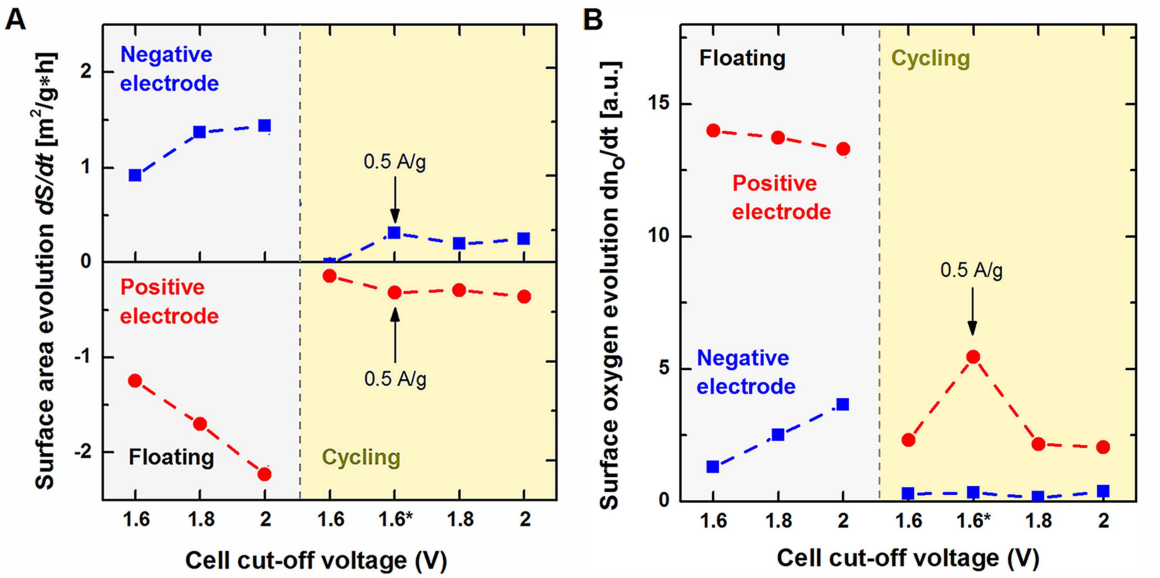

Figure 3. (A) Comparison of dS/dt (S_{BET} changes normalized with time) and (B) dn_O/dt (oxygen content changes of carbon electrode normalized with time) for positive and negative electrodes aged during floating and cycling conditions, respectively. All galvanostatic cycling tests are at a specific current of 0.2 A/g, except the 1.6 V* with 0.5 A/g.

assumed constant) according to Equation 1. The average gas generation rate Δn is a result of voltage-dependent side-reactions and is thus expected to have an exponential dependence on the cell voltage V according to the Tafel-equation:

$$\Delta p_{avg} \sim \Delta n \frac{RT}{Vol} \sim Ae^{B \bullet V} \quad (1)$$

The two empirical parameters A and B may thus be extracted from a fit of Equation 1 to Δp^F (Figure 2B, dashed black line, $R^2 = 0.98$, $A = 2.3.10^{-13}$ bar/min, and $B = 11.1\ V^{-1}$). Thereby, the voltage dependence of the gas generation mechanism during the floating step may be acquired and compared to the gas generation rate during the cycling sequence Δp^C. Figure 2B shows the expected pressure increase rates (C Expected, in grey) if the gas generation mechanism during the cycling step would have an identical voltage-dependence as the gas generation mechanism during the floating step. In fact, when their respective voltage dependencies are accounted for, the average gas generation rate during a cycling step is significantly higher than during a floating step. A partial explanation for the higher gas generation rate during cycling is the reformation of the carbon surface groups (< 0.6 V) occurring in every cycle – a dynamic process that does not occur during a voltage hold. However, voltage floating at high cell polarization is significantly more efficient in generating gas per time unit (Figure 2A), thus explaining the poorer performance of EDLCs subjected to floating conditions. In conclusion, despite the observation that the electrochemical cycling is harsher on the EDLC (when the average gas evolution rate is normalized with respect to applied average voltage), the electrochemical floating at the cut-off voltage leads to a more rapid internal pressure build-up and earlier failure of the EDLC.

Ex-situ textural and chemical analysis of the carbon electrodes were performed in order to further evaluate the impact of EDLC ageing under cycling and floating conditions. Figure 3A shows the time-normalized change dS_{BET}/dt in the specific surface areas of the positive and negative carbon electrodes. The pristine carbon electrodes have a large specific BET surface area of 1722 m^2/g and a total pore volume V_{total} of 0.72 cm^3/g, which almost exclusively consist of micropores ($V_{micro} \sim 0.71\ cm^3/g$). Regardless of the applied electrochemical ageing conditions, the surface area of the negative electrodes consistently increased whereas the area of the positive electrode decreased. Previous studies[47,51,56–58] confirmed that carbon negative electrode prefers to operate around hydrogen evolution equilibrium potential. Hydrogen electrosorption enhances the capacitance value by pseudocapacitive effects[59–63] and enforces the positive electrode to operate at higher potentials in order to balance the additional charge accumulated in negative electrode. Nonetheless, electrolyte reduction (occurring after exceeding the hydrogen storage capacity) at the negative electrode (e.g. $H_2O + e^- \rightarrow {}^1/_2H_2 + OH^-$) leads apart from H_2 evolution to the formation of an alkaline environment[47,64–65] with highly active and mobile OH^- specimen.[66] pH measured for the electrolyte extracted from the negative electrode was in fact alkaline (ranging from 9.8 to 11.4, interestingly, the pH measured depended on the final voltage, not the procedure), while for positive electrode almost no change was observed (ca. 5.2 *vs.* 5.9 for initial solution). Chemical activation methods have been widely employed in modifying the textural and chemical characteristics of activated carbons during carbonisation process.[67–73] Alkali metals are well-known to develop the microporosity during an activation process. In our case, we

believe that the *in-situ* formation of either LiOH or $[Li^+][OH^-]$ promotes the increase in the negative electrode surface area by 'alkaline activation'; alkaline electrolyte has better tendency for micropore filling (lower surface tension) and thus the ions might penetrate the pores inaccessible in neutral environment. This idea might be supported by our observation during *operando* Raman experiments reported earlier: deformation of D bands during negative polarization in hydrogen evolution potential region suggested reversible hydrogen adsorption (confirmed by signals observed for C–H bonds) with charge transfer process.[51] Furthermore, slight change in Raman shift for D band, accompanied by the increase of secondary reflections (2D) intensity indicate a change in the distance between graphene layers (or number of defects) in the electrode. On the macroscopic scale, this would result in increase of the surface area of the electrode. In contrast to our observation, Cericola et al. assumed that H_2 evolution from the negative electrode could block the pores and result in the loss of S_{BET}.[45] However, in their study, decomposition of water contamination (~1000 ppm) in organic electrolyte (Et_4NBF_4 in propylene carbonate) possess certainly dissimilar chemical environment as the aqueous system. On the positive electrode, carbon surface group oxidation (e.g. $(RCO)_2O–4e^- \rightarrow 2R + CO\uparrow + CO_2\uparrow$, $U > 0.6$ V) and carbon corrosion (e.g. $C + 2H_2O–4e^- \rightarrow CO/CO_2\uparrow + 4H^+$, $U > 1.6$ V) are two dominating processes[47] which both rather appear to cause a reduction in the electrode surface area. In this place, we would like to point out that one should pay special attention in the cell configuration and possible sources of gas evolution in the system. It appears that once current collector is fully covered by the electrode material, hydrogen evolution overpotential is high and the process occurs with the hydrogen electrosorption as a subsequent step. However, once the current collector faces directly the electrolyte, hydrogen is easily evolved on the surface and might have a detrimental effect on the electrode. Although the 'hydrogen corrosion' is not the case for noble current collectors,[74–78] in case of stainless steel (316L and 304SU), it might additionally promote formation of protective layer[79–85] and then introduce another resistance to the system (observed most likely as ESR but also EDR increase). Interestingly, the postulated LiOH formation might also play a role in this process.[86] The performance decay during ageing, as observed in Figure 1, could therefore be largely governed by carbon corrosion induced surface area loss at the positive electrode.[42] Figure 3A further shows that the electrochemical floating conditions always had a much stronger impact on *dS/dt* than the cycling conditions, even when the average voltage difference is taken into consideration. Following the same line of argumentation as above, the more rapid performance loss induced by the voltage floating (compare Figure 1A and B) could thus also be explained by the more extensive surface area loss of the positive electrode during floating than during cycling. Holding the voltage for an extended time most likely creates a more persistent chemical environment at negative (alkaline) and positive (acidic) electrodes, hence providing a more efficient weathering of the carbons.

Interestingly, irrespective of the floating/cycling conditions, the negative electrode displays an inverse exponential increase in surface area with cut-off voltage whereas the positive electrode displays a corresponding linear decrease (Figure 3A, and Figure S4A). This observation is in line with the potential profiles of the electrodes in the symmetric system reported previously[51] and indicates that once negative electrode reaches the hydrogen storage region, positive electrode balances it by elevating linearly the operating potential. This results in continuous electrode oxidation (boosted at higher system voltages). Furthermore, when the overpotential $\eta \ll RT/zF$, one can get the proportional relation of $dS/dt \sim j \sim k\eta$ ($k = j_0 \cdot zF/RT$) according to the approximation of Butler-Volmer equation. The linear decrease on the positive side indicates a different electrochemical kinetics compared with the negative electrode. A higher applied current during cycling does however appear to increase the extent of side-reactions, and as a consequence also the *dS/dt* after cycling (0.5 A/g, Figure 3A). Furthermore, worth noting is that changes in total pore volume *dV/dt* follow the same trend as the surface area (compare Figure 3A and Figure S4B in Supp. info). Naturally, the surface area and volume of the micropores are intimately related.

Figure 3B shows the evolution of the surface oxygen content with respect to cut-off voltage during the floating and cycling conditions. Irrespective of the ageing conditions, the positive electrode possesses a 4–5 times higher oxygen content compared to the negative electrode. Surface oxygenation/oxidation is an intermediate reaction step in the carbon corrosion process that occurs predominantly on the positive electrode during high cell polarizations.[47] Increased number of surface oxygen-based functionalities is also observed on the negative electrode with higher cut-off voltages due to potential-activated electrolyte degradation. Oxygen radicals $O^{\cdot}$/$HO^{\cdot}$ formed at the positive electrode could partly contribute to the oxygenation of the negative electrode by diffusing across the separator. The lower/higher increase in oxygen content of the positive/negative electrode with higher cut-off voltage can largely be explained by the accompanying reduction/increase of surface area (Figure 3A).

The amount of oxygen increased much more significantly during floating than during cycling, which again can be explained by the formation of a harsher alkaline/acidic environment at the negative/positive electrode during floating. Interestingly, the oxygen content of the positive electrode increased more significantly under higher current conditions (0.5 A/g), which could be related to the observation that electrolyte degradation rate is significantly higher during cycling than during floating at a cut-off voltage of 1.6 V (compare *dP/dt* in Figure S2A,B).

3. Conclusions

Aqueous EDLCs based on 1 mol/L Li_2SO_4 electrolyte and activated carbon electrodes were tested under both galvanostatic cycling and voltage holding. Ageing aspects including capacitance loss, EDR/ESR increase, variation of active surface

areas, modification of surface functionalities, pressure build-up, and gas evolution are characterized and analysed by *post-mortem* and *operando* techniques. The major findings are summarized as following:

1. Specific surface area of carbon electrode (+) is decreasing during the galvanostatic cycling or the voltage holding process. In contrast, an increase of surface area occurs on the carbon electrode on the negative side (−).
2. Hydrogen sorption or hydrogen evolution on the negatively polarized electrode results in the formation of OH^-, which serves as the activating agent for the development of porous structure. Thus, the negatively polarized electrode possesses an increased micropore volume V_{micro}.
3. Carbon corrosion is evidenced by the increased oxygen content of carbon electrode, carbon loss, and CO/CO_2 gas evolution.
4. Ageing phenomena, i.e., active surface loss, carbon oxidation, carbon corrosion, capacitance fading, cell impedance increase, and gas evolution, are accelerated at higher cell polarization $U > 1.6$ V. Repeated cycling appears to assist the depletion of oxygen species from the positively polarized electrode, especially in the mild cycling conditions, i.e., $U <$ 1.6 V.
5. Degradation processes of different nature occur on positively polarized carbon electrodes: Floating = direct carbon corrosion, Galvanostatic Cycling = reformation of surface groups combined with carbon corrosion.
6. In general, time efficiency of ageing is higher for floating compared to cycling test. Repeated sequences combining a short-term cycling and a long-term voltage holding is recommended for speeding up the lifetime evaluation of EDLCs (until 80% capacitance retention). Caution shall be taken to replace the conventional cycling test by other testing procedures completely.

Acknowledgements

Financial support from the Polish-Swiss Research Programme (INGEC PSPB-107/2010) and European Research Council within the Starting Grant project (GA 759603) under European Unions' Horizon 2020 research and innovation programme are gratefully acknowledged.

Conflict of Interest

The authors declare no conflict of interest.

Keywords: aqueous supercapacitors · cell ageing · cycling tests · high voltage · voltage holding

[1] M. Winter, R. J. Brodd, *Chem. Rev.* **2004**, *104*, 4245.
[2] P. Simon, Y. Gogotsi, B. Dunn, *Science* **2014**, *343*, 1210.
[3] R. Kötz, M. Carlen, *Electrochim. Acta* **2000**, *45*, 2483.
[4] P. Kurzweil, in *Electrochemical Energy Storage for Renewable Sources and Grid Balancing*, DOI: 10.1016/b978-0-444-62616-5.00019-x, **2015**, pp. 345.
[5] J. R. Miller, A. F. Burke, *Electrochem. Soc. Interface* **2008**, *17*, 53.
[6] N. S. Choi, Z. Chen, S. A. Freunberger, X. Ji, Y. K. Sun, K. Amine, G. Yushin, L. F. Nazar, J. Cho, P. G. Bruce, *Angew. Chem. Int. Ed.* **2012**, *51*, 9994.
[7] Y. Zhai, Y. Dou, D. Zhao, P. F. Fulvio, R. T. Mayes, S. Dai, *Adv. Mater.* **2011**, *23*, 4828.
[8] S. Trasatti, P. Kurzweil, *Platinum Met. Rev.* **1994**, *38*, 46.
[9] A. Vlad, A. Balducci, *Nat. Mater.* **2017**, *16*, 161.
[10] J. Y. Hwang, M. F. El-Kady, M. Li, C. W. Lin, M. Kowal, X. Han, R. B. Kaner, *Nano Today* **2017**, *15*, 15.
[11] Y. Gogotsi, *ACS Nano* **2014**, *8*, 5369.
[12] J. P. Zheng, *J. Electrochem. Soc.* **2003**, *150*, A484.
[13] M. Sevilla, R. Mokaya, *Energy Environ. Sci.* **2014**, *7*, 1250.
[14] W. W. C. Chan, P. T. Hammond, S. Glotzer, M. C. Hersam, Y. Gogotsi, A. Javey, J. H. Hafner, C. R. Kagan, A. Khademhosseini, R. M. Penner, N. A. Kotov, A. L. Rogach, S. T. Lee, R. E. Schaak, H. Mohwald, M. M. Stevens, P. A. Mulvaney, A. T. S. Wee, A. E. Nel, C. G. Willson, P. J. Nordlander, H. L. Tierney, W. J. Parak, P. S. Weiss, *ACS Nano* **2015**, *9*, 11503.
[15] F. Béguin, E. Frąckowiak, *Carbons for Electrochemical Energy Storage and Conversion Systems*, **2009**.
[16] C. Liu, F. Li, L. P. Ma, H. M. Cheng, *Adv. Mater.* **2010**, *22*, E28.
[17] F. Beguin, V. Presser, A. Balducci, E. Frackowiak, *Adv. Mater.* **2014**, *26*, 2219.
[18] C. Zhong, W. Hu, *Electrolytes for Electrochemical Supercapacitors*, **2016**.
[19] V. Khomenko, E. Raymundo-Piñero, F. Béguin, *J. Power Sources* **2008**, *177*, 643.
[20] P. Jezowski, K. Fic, O. Crosnier, T. Brousse, F. Beguin, *J. Mater. Chem. A* **2016**, *4*, 12609.
[21] K. Naoi, P. Simon, *Journal of The Electrochemical Society (JES)* **2008**, 17, 34.
[22] K. Naoi, Y. Nagano, in *Supercapacitors*, DOI: 10.1002/9783527646661.ch7 (Ed: F. Beguin) **2013**, Ch. 7, pp. 239.
[23] K. Naoi, W. Naoi, S. Aoyagi, J.-I. Miyamoto, T. Kamino, *Acc. Chem. Res.* **2013**, *46*, 1075.
[24] K. Fic, A. Platek, J. Piwek, E. Frackowiak, *Mater. Today* **2018**, *21*, 437.
[25] Y. Gogotsi, P. Simon, *Science* **2011**, *334*, 917.
[26] G. Z. Chen, *Int. Mater. Rev.* **2017**, *62*, 173.
[27] M. Jiang, J. Zhu, C. Chen, Y. Lu, E. S. Pampal, L. Luo, P. Zhu, X. Zhang, *J. Mater. Chem. A* **2016**, *4*, 16588.
[28] B. Akinwolemiwa, C. Peng, G. Z. Chen, *J. Electrochem. Soc.* **2015**, *162*, A5054.
[29] R. Kötz, P. W. Ruch, D. Cericola, *J. Power Sources* **2010**, *195*, 923.
[30] C.-L. Liu, W. Dong, G. Cao, J. Song, L. Liu, Y. Yang, *J. Electrochem. Soc.* **2008**, *155*, F1.
[31] O. Barbieri, M. Hahn, A. Herzog, R. Kotz, *Carbon* **2005**, *43*, 1303.
[32] L. Guan, L. Yu, G. Z. Chen, *Electrochim. Acta* **2016**, *206*, 464.
[33] W. Gu, G. Yushin, *Wiley Interdisciplinary Reviews-Energy and Environment* **2014**, *3*, 424.
[34] H. Ji, X. Zhao, Z. Qiao, J. Jung, Y. Zhu, Y. Lu, L. L. Zhang, A. H. MacDonald, R. S. Ruoff, *Nat. Commun.* **2014**, *5*.
[35] O. Bohlen, J. Kowal, S. Dirk Uwe, *J. Power Sources* **2007**, *173*, 626.
[36] A. M. Bittner, M. Zhu, Y. Yang, H. F. Waibel, M. Konuma, U. Starke, C. J. Weber, *J. Power Sources* **2012**, *203*, 262.
[37] P. Azaïs, L. Duclaux, P. Florian, D. Massiot, M. A. Lillo-Rodenas, A. Linares-Solano, J. P. Peres, C. Jehoulet, F. Béguin, *J. Power Sources* **2007**, *171*, 1046.
[38] N. Omar, H. Gualous, J. Salminen, G. Mulder, A. Samba, Y. Firouz, M. A. Monem, P. Van den Bossche, J. Van Mierlo, *J. Appl. Electrochem.* **2014**, *44*, 509.
[39] Q. Abbas, F. Béguin, *J. Power Sources* **2016**, *318*, 235.
[40] D. Weingarth, A. Foelske-Schmitz, R. Kötz, *J. Power Sources* **2013**, *225*, 84.
[41] O. Bohlen, J. Kowal, D. U. Sauer, *J. Power Sources* **2007**, *172*, 468.
[42] P. Ratajczak, K. Jurewicz, P. Skowron, Q. Abbas, F. Béguin, *Electrochim. Acta* **2014**, *130*, 344.
[43] A. Bello, F. Barzegar, M. J. Madito, D. Y. Momodu, A. A. Khaleed, T. M. Masikhwa, J. K. Dangbegnon, N. Manyala, *Electrochim. Acta* **2016**, *213*, 107.
[44] P. W. Ruch, D. Cericola, A. Foelske-Schmitz, R. Kötz, A. Wokaun, *Electrochim. Acta* **2010**, *55*, 4412.
[45] D. Cericola, P. W. Ruch, A. Foelske-Schmitz, D. Weingarth, R. Kötz, *International Journal of Electrochemical Science* **2011**, *6*, 988.

[46] P. Ratajczak, K. Jurewicz, F. Beguin, *J. Appl. Electrochem.* **2014**, *44*, 475.
[47] M. He, K. Fic, E. Frąckowiak, P. Novák, E. J. Berg, *Energy Environ. Sci.* **2016**, *9*, 623.
[48] B. Avasarala, R. Moore, P. Haldar, *Electrochim. Acta* **2010**, *55*, 4765.
[49] M. Zhu, C. J. Weber, Y. Yang, M. Konuma, U. Starke, K. Kern, A. M. Bittner, *Carbon* **2008**, *46*, 1829.
[50] M. He, K. Fic, E. Frąckowiak, P. Novák, E. J. Berg, *Energy Storage Mater.* **2016**, *5*, 111.
[51] K. Fic, M. He, E. J. Berg, P. Novak, E. Frackowiak, *Carbon* **2017**, *120*, 281.
[52] J. Jagiello, J. P. Olivier, *Carbon* **2013**, *55*, 70.
[53] J. Jagiello, J. P. Olivier, *Adsorption-Journal of the International Adsorption Society* **2013**, *19*, 777.
[54] M. He, E. Castel, A. Laumann, G. Nuspl, P. Novak, E. J. Berg, *J. Electrochem. Soc.* **2015**, *162*, A870.
[55] M. He, L. Boulet-Roblin, P. Borel, C. Tessier, P. Novák, C. Villevieille, E. J. Berg, *J. Electrochem. Soc.* **2016**, *163*, A83.
[56] Q. Abbas, P. Ratajczak, P. Babuchowska, A. L. Comte, D. Belanger, T. Brousse, F. Beguin, *J. Electrochem. Soc.* **2015**, *162*, A5148.
[57] J. H. Chae, G. Z. Chen, *Electrochim. Acta* **2012**, *86*, 248.
[58] M. P. Bichat, E. Raymundo-Piñero, F. Béguin, *Carbon* **2010**, *48*, 4351.
[59] F. Béguin, M. Friebe, K. Jurewicz, C. Vix-Guterl, J. Dentzer, E. Frackowiak, *Carbon* **2006**, *44*, 2392.
[60] G. Lota, K. Fic, K. Jurewicz, E. Frackowiak, *Central European Journal of Chemistry* **2011**, *9*, 20.
[61] K. Jurewicz, E. Frackowiak, F. Béguin, *Appl. Phys. A* **2004**, *78*, 981.
[62] F. Beguin, K. Kierzek, M. Friebe, A. Jankowska, J. Machnikowski, K. Jurewicz, E. Frackowiak, *Electrochim. Acta* **2006**, *51*, 2161.
[63] K. Babel, D. Janasiak, K. Jurewicz, *Carbon* **2012**, *50*, 5017.
[64] K. Fic, E. Frackowiak, F. Beguin, *J. Mater. Chem.* **2012**, *22*, 24213.
[65] Q. Gao, L. Demarconnay, E. Raymundo-Piñero, F. Béguin, *Energy Environ. Sci.* **2012**, *5*, 9611.
[66] V. Grozovski, S. Vesztergom, G. G. Láng, P. Broekmann, *J. Electrochem. Soc.* **2017**, *164*, E3171.
[67] A. Kumar, H. M. Jena, *Results in Physics* **2016**, *6*, 651.
[68] X. Wang, N. Gao, Q. Zhou, H. Dong, H. Yu, Y. Feng, *Bioresour. Technol.* **2013**, *144*, 632.
[69] C. Portet, M. A. Lillo-Rodenas, A. Linares-Solano, Y. Gogotsi, *Phys. Chem. Chem. Phys.* **2009**, *11*, 4943.
[70] B. Xu, F. Wu, Y. Su, G. Cao, S. Chen, Z. Zhou, Y. Yang, *Electrochim. Acta* **2008**, *53*, 7730.
[71] F. C. Wu, R. L. Tseng, R. S. Juang, *J. Colloid Interface Sci.* **2005**, *283*, 49.
[72] K. Kierzek, E. Frackowiak, G. Lota, G. Gryglewicz, J. Machnikowski, *Electrochim. Acta* **2004**, *49*, 515.
[73] M. J. Bleda-Martinez, J. A. Macia-Agullo, D. Lozano-Castello, E. Morallon, D. Cazorla-Amoros, A. Linares-Solano, *Carbon* **2005**, *43*, 2677.
[74] M. Pourbaix, *Corros. Sci.* **1974**, *14*, 25.
[75] T. Ohmori, M. Enyo, *Electrochim. Acta* **1992**, *37*, 2021.
[76] Y. Xu, *Int. J. Hydrogen Energy* **2009**, *34*, 77.
[77] T. Fujitani, I. Nakamura, T. Akita, M. Okumura, M. Haruta, *Angew. Chem. Int. Ed.* **2009**, *48*, 9515.
[78] N. Pentland, J. O. M. Bockris, E. Sheldon, *J. Electrochem. Soc.* **1957**, *104*, 182.
[79] Y. F. Cheng, *Electrochim. Acta* **2007**, *52*, 2661.
[80] D. M. Grant, D. L. Cummings, D. A. Blackburn, *J. Nucl. Mater.* **1988**, *152*, 139.
[81] V. Cicek, *Corrosion Engineering*, **2014**.
[82] P. T. Jakobsen, E. Maahn, *Corros. Sci.* **2001**, *43*, 1693.
[83] J. M. Olivares-Ramírez, M. L. Campos-Cornelio, J. Uribe Godínez, E. Borja-Arco, R. H. Castellanos, *Int. J. Hydrogen Energy* **2007**, *32*, 3170.
[84] M. Li, L. Q. Guo, L. J. Qiao, Y. Bai, *Corros. Sci.* **2012**, *60*, 76.
[85] E. Remita, B. Tribollet, E. Sutter, V. Vivier, F. Ropital, J. Kittel, *Corros. Sci.* **2008**, *50*, 1433.
[86] I. M. Svishchev, R. A. Carvajal-Ortiz, K. I. Choudhry, D. A. Guzonas, *Corros. Sci.* **2013**, *72*, 20.

Manuscript received: August 20, 2018
Accepted manuscript online: October 16, 2018
Version of record online: November 7, 2018